



Trade Science Inc.

Materials Science

An Indian Journal

Full Paper

MSAIJ, 9(4), 2013 [138-143]

Effect of precipitant on micrograph and luminescent properties of $Gd_2O_3:Eu^{3+}$ synthesized by the hydrothermal method

Yong Qing Zhai*, Li Li Wang, Juan Chen, Ya Hong Liu, Xiao Na Li

College of Chemistry and Environmental Science, Hebei University, Baoding 071002, (P.R. CHINA)

E-mail: zhaiyongqinghbu@163.com

ABSTRACT

$Gd_2O_3:Eu^{3+}$ phosphors were synthesized by hydrothermal method using aqueous ammonia and ammonium bicarbonate as the precipitation agents respectively. TG-DTA, FT-IR and XRD were used to analyze the thermal decomposition behavior of hydrothermal precursors and the formation process of target product. SEM was used to characterize the micrograph of phosphors. Fluorescence spectrophotometer was used to investigate the luminescent properties of phosphors. The results show that the hydrothermal precursors are $Gd(OH)_3$ and $Gd_2(CO_3)_3 \cdot xH_2O$ respectively for aqueous ammonia and ammonium bicarbonate as precipitants. $Gd_2O_3:Eu^{3+}$ crystallites with pure cubic phase can be obtained after the precursors were calcined at 800 °C for 2 h. The morphology of $Gd_2O_3:Eu^{3+}$ is affected by the precipitant. The main excitation peak of as-synthesized $Gd_2O_3:Eu^{3+}$ crystallite is at 261 nm, attributed to the charge transfer state of Eu-O. The main emission peak is at 613 nm, which is ascribed to the transition of $^5D_0 \rightarrow ^7F_2$ of Eu^{3+} , resulting in a red emission. The luminescent intensity of the sample using ammonium bicarbonate as the precipitant is relatively strong. © 2012 Trade Science Inc. - INDIA

KEYWORDS

$Gd_2O_3:Eu^{3+}$;
Precipitant;
Hydrothermal synthesis;
Micrograph.

INTRODUCTION

Rare-earth luminescent materials have been applied widely in many fields due to their excellent properties, and have become a research hotspot in the luminous field at present^[1]. Gd_2O_3 is a kind of matrix materials with high performance and easily obtained. Eu^{3+} -doped Gd_2O_3 phosphor has higher luminous efficiency and better spectral characteristics, so it is a kind of high efficient red phosphors. It has been used in high definition television, flat panel display, green lighting project, and other fields. Therefore, it received extensive atten-

tion^[2-4]. The luminous property of rare earth materials is related closely to their structure and morphology. In recent year, $Gd_2O_3:Eu^{3+}$ phosphors with different morphology were prepared by different methods. For example, Liu et al^[5] synthesized spherical and hollow $Gd_2O_3:Eu^{3+}$ phosphors by homogeneous precipitation and hydrothermal method Li et al^[6] synthesized $Gd_2O_3:Eu^{3+}$ nanowires with a diameter of 100nm by AAO template method, but the size of nanowires was limited by the used template, and the template is difficult to be removed; Zhang et al^[7] synthesized uniform $Gd_2O_3:Eu^{3+}$ nanorods by surfactant (PEG)-as-

sisted hydrothermal method using NaOH as precipitant, but NaOH is very expensive and has strong corrosion, and Na^+ is difficult to be removed.

In our present work, cheap ammonia and ammonium bicarbonate were used as the precipitants respectively, $\text{Gd}_2\text{O}_3:\text{Eu}^{3+}$ phosphors were synthesized by hydrothermal method using PEG as the surfactant. The effect of precipitants on the structure of the precursor and the target product, micrograph of the target product, and luminescent properties were investigated.

EXPERIMENTAL

Synthesis of $\text{Gd}_2\text{O}_3:\text{Eu}^{3+}$

Gd_2O_3 (99.99%), Eu_2O_3 (99.99%), nitric acid (65%, A.R.), ammonium hydroxide (25%, A.R.) and ammonium bicarbonate (A.R.) were used as the starting materials. Polyethylene glycol (PEG, molecular weight=1000, A.R.) used as surfactant.

The detailed procedure was as follows: First, Gd_2O_3 and Eu_2O_3 were dissolved respectively in a certain amount of hot nitric acid to form $\text{Gd}(\text{NO}_3)_3$ and $\text{Eu}(\text{NO}_3)_3$ aqueous solutions. The accurate concentration of $\text{Gd}(\text{NO}_3)_3$ and $\text{Eu}(\text{NO}_3)_3$ solutions was determined by EDTA complexing titrimetry. They are 0.2897 mol/L and 0.0923 mol/L respectively. Second, 26.51 mL $\text{Gd}(\text{NO}_3)_3$ and 3.47 mL $\text{Eu}(\text{NO}_3)_3$ were mixed together with a certain amount of PEG as surfactant under constant stirring. Then ammonium hydroxide was dropped slowly into the above solution to adjust the pH value to 3 ~ 4. Third, 2 mol/L aqueous ammonia or ammonium bicarbonate aqueous as precipitant was dropped into the solution under violent stirring, and the pH value was kept at about 8. After stirring for 1 h, the mixture was transferred into a Teflon-lined stainless steel autoclave with a filling capacity of 70%; hydrothermal reaction was carried out at 180° for 24 h, and then cooled to room temperature. The obtained suspension was filtered and washed with distilled water and a little amount of alcohol. The obtained precursor was put into an oven and dried at 70 °C for 4 h. Finally, this precursor was calcined in a muffle furnace at 800 °C for 2 h in air to obtain the oxide phosphors.

Characterization

IR spectrum was recorded as KBr pellets on Nicolet

380 Fourier transform infrared spectrometer. Phases and crystallization of samples were identified by X-ray powder diffraction (XRD) with a Y2000 diffractometer with $\text{Cu K}\alpha$ radiation (20 kV×30 mA) and $\lambda=0.154060$ nm. The particle size and morphology of the samples were characterized with a JSM-7500F scanning electron microscopy (SEM). The excitation and emission spectra of the samples were recorded on a F-380 fluorescence spectrophotometer. For comparison of the phosphors, the excitation and emission spectra were measured with the same instrument parameters. The emission spectra were excited at the wavelength of the highest peak of excitation spectrum. All samples were determined at room temperature.

RESULTS AND DISCUSSIONS

FTIR analysis

The FT-IR spectra of the precursor and the sample obtained at 800 °C for 2 h by using aqueous ammonia as precipitant are shown in Figure 1. In Figure 1 (a), the absorption peak near 3610 cm^{-1} is due to -OH stretching vibration of H_2O ; the absorption peaks at 3734 cm^{-1} and 3172 cm^{-1} are caused by NH_4^+ absorbed on the surface of the particles; the absorption peak near 1402 cm^{-1} is due to NO_3^- , which shows that trace of NO_3^- still exists in the precursor; the weak absorption peak near 1179 cm^{-1} is due to CO_2 in the air; the strong near 708 cm^{-1} is ascribed to the vibration of Gd-OH, which proves that the precursor is $\text{Gd}(\text{OH})_3$. From Figure 1 (b), it can be seen that the above characteristic bands have almost disappeared after the precursor is calcined at 800 °C. The strong absorption peaks at 545 cm^{-1} and 440 cm^{-1} are due to Gd-O stretching vibration in Gd_2O_3 phase, which proves that Gd_2O_3 has been formed.

Figure 2 shows that the FT-IR spectra of the precursor and the sample obtained at 800 °C for 2 h by using ammonium bicarbonate as precipitant. In Figure 2(a), the broad absorption band near 3404 cm^{-1} is due to -OH group of H_2O , which shows that the precursor has a certain amount of crystal water; the absorption peak at 3179 cm^{-1} is attributed to NH_4^+ absorbed on the surface of the particles; the absorption peak at 1401 cm^{-1} is caused by NO_3^- ; the absorption peaks at 1616

Full Paper

cm^{-1} , 1495 cm^{-1} , 835 cm^{-1} , 758 cm^{-1} and 686 cm^{-1} are ascribed to the stretching and bending vibration of CO_3^{2-} . These prove that the precursor is hydrated gadolinium carbonate ($Gd_2(CO_3)_3 \cdot xH_2O$). From Figure 2 (b), it can be seen that the characteristic peaks of $-OH$ and CO_3^{2-} have disappeared after the precursor is calcined at $800\text{ }^\circ\text{C}$, but a small amount of CO_2 and NO_3^- has

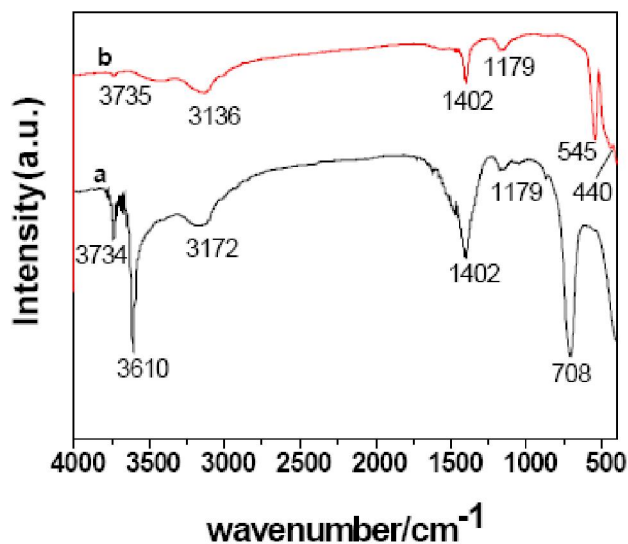


Figure 1 : IR spectra of the precursor (a) and the calcined sample (b) using aqueous ammonia as the precipitant

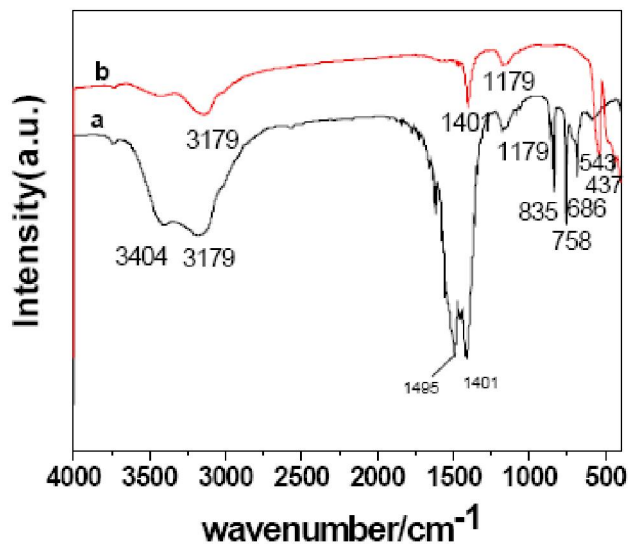


Figure 2 : IR spectra of the precursor (a) and the calcined sample (b) using ammonium bicarbonate as the precipitant

not been removed completely, mainly due to the absorbed CO_2 in the air^[8]. The strong absorption peaks at 543 cm^{-1} and 437 cm^{-1} are due to Gd-O stretching vibration in Gd_2O_3 phase, which proves that hydrated gadolinium carbonate has been transformed into Gd_2O_3 .

XRD patterns

Figure 3 shows the X-ray diffraction patterns of the hydrothermal precursors obtained by using aqueous ammonia as the precipitant and the sample obtained by calcining the precursor at $800\text{ }^\circ\text{C}$ for 2h. As shown in Figure 3(a), the X-ray diffraction peaks are in good agreement with powder data in JCPDS card No.83-2037. According to that, the precursor is hexagonal $Gd(OH)_3$, which is consistent with the result of FTIR analysis. In Figure 3 (b), all the X-ray diffraction peaks can be indexed to cubic Gd_2O_3 (JCPDS No.12-0797). In this pattern, the peaks of compounds of Eu cannot be found, which indicates that Eu^{3+} ions have entered into the host lattice and have little effect on the crystal

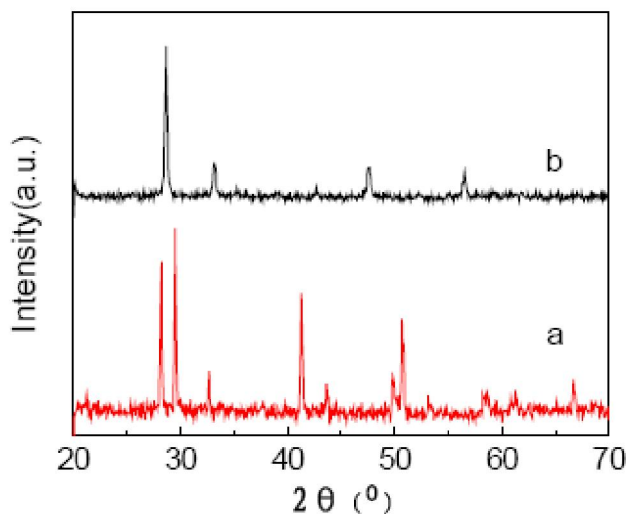


Figure 3 : XRD patterns of the precursor (a) and the calcined sample (b) using aqueous ammonia as the precipitant

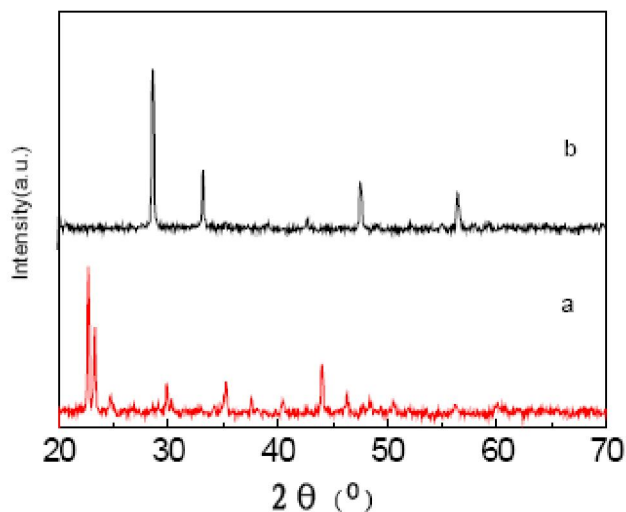


Figure 4 : XRD patterns of the precursor (a) and the calcined sample (b) using ammonium bicarbonate as the precipitant

structure of the host Gd_2O_3 . The strong and sharp diffraction peaks show that as-synthesized $Gd_2O_3:Eu^{3+}$ has better crystallinity.

Figure 4 shows the X-ray diffraction patterns of the hydrothermal precursors obtained by using ammonium bicarbonate as the precipitant and the sample obtained by calcining the precursor at 800 °C for 2h. In Figure 4(a), the X-ray diffraction peaks can be assigned to orthorhombic $Gd_2(CO_3)_3 \cdot xH_2O$ phase (JCPDS No. 37-0559), which is consistent with the result of FTIR analysis. In Figure 4 (b), the X-ray diffraction peaks of sample are in excellent accordance with the powder data in JCPDS card No. 12-0797, indicating that the calcined sample is cubic $Gd_2O_3:Eu^{3+}$.

According to the results, the kind of precipitant affects the phase structure of the precursor significantly, but has little effect on the phase structure of the calcined sample. Comparing Figure 3 (b) with Figure 4 (b), it can be found the diffraction peaks of as-synthesized $Gd_2O_3:Eu^{3+}$ using ammonium bicarbonate as the precipitant are stronger and sharper than those using aqueous ammonia as the precipitant, which indicates that the crystallization of $Gd_2O_3:Eu^{3+}$ obtained by using ammonium bicarbonate as the precipitant is more perfect.

SEM analysis of $Gd_2O_3:Eu^{3+}$ powder

The micrograph of the $Gd_2O_3:Eu^{3+}$ powder prepared with different precipitants was observed by SEM and shown in Figure 5.

As shown in Figure 5 (a), while using aqueous ammonia as the precipitant, the micrograph of $Gd_2O_3:Eu^{3+}$ presents short bar in shape with small slenderness ratio and relatively uniform size, the diameter is about 100 nm~500 nm and the length is about 300 nm~1 μ m. From Figure 5 (b), it can be noted that the micrograph of $Gd_2O_3:Eu^{3+}$ obtained by using ammonium bicarbonate as the precipitant shows long strips in shape with big slenderness ratio, the diameter is about 100 nm~1 μ m and the length is about 1~9 μ m. Therefore, the type of precipitants is an important factor for the morphology of $Gd_2O_3:Eu^{3+}$. The reason is that the alkaline of aqueous ammonia is much stronger than ammonium bicarbonate, which significantly improves the opportunity and the rate of nucleation in the precipitation process, so the grain size of $Gd_2O_3:Eu^{3+}$ is smaller. Com-

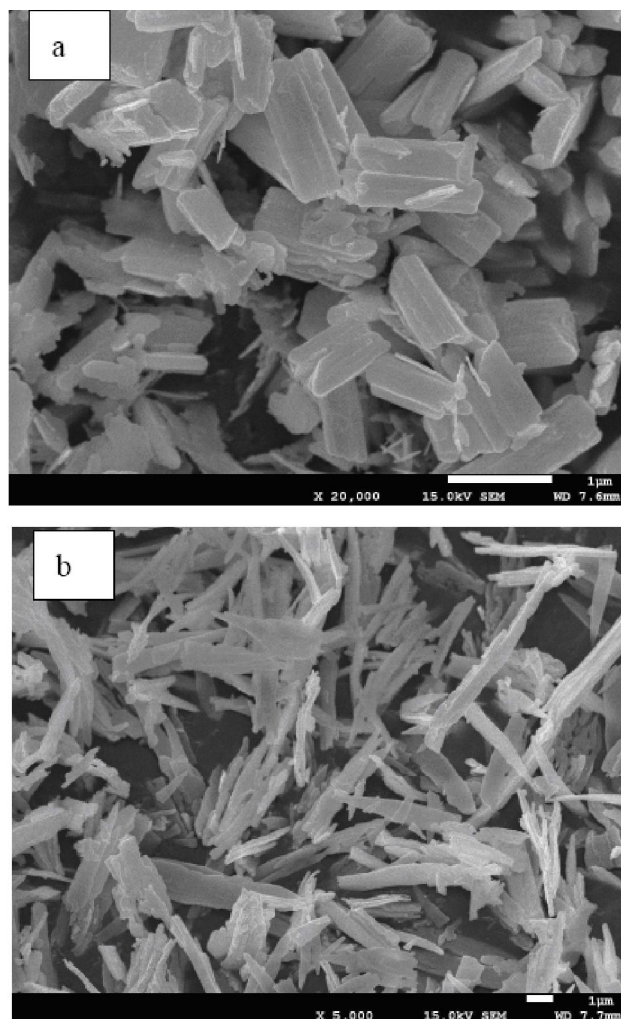


Figure 5 : SEM images of samples in the presence of different precipitation agents (a) Aqueous ammonia and (b) ammonium bicarbonate

pared with the ammonia as precipitant, the grain size of sample obtained by using ammonium hydrogen carbonate as the precipitant is relatively bigger, but the degree of reunion for the calcined particles is significantly reduced, and the dispersion is relatively better, it is due to the production of CO_2 from CO_3^{2-} in the process of the reaction and roasting, which can greatly inhibit the agglomeration of the particles.

Photoluminescence properties

Under ultraviolet (UV) radiation at 254nm, the samples show bright red-emitting. Figure 6 shows the excitation spectra (monitored at 613nm) of the samples $Gd_2O_3:Eu^{3+}$ obtained respectively by using aqueous ammonia and ammonium bicarbonate as the precipitants. As shown in Figure 8, the excitation spectrum is

Full Paper

composed of two major parts: (1) the wide band between 200 nm and 300 nm, which is assigned to the charge-transfer-state (CTS) of $Eu^{3+}-O^{2-}$, i.e., the coordination O^{2-} transfers an electron from the 2p orbit to the 4f orbit of Eu^{3+} in coordination center, the strongest excitation peak is at about 261 nm, the shoulder peak at about 277 nm is ascribed to the transition of ${}^6S_{7/2}-{}^6I_7$ of Gd^{3+} . (2) a series of weak excitation peaks between 300 nm and 350 nm, attributed to the higher energy level ${}^7F_0 \rightarrow {}^5D_{3,4}$ transition of Eu^{3+} . Compared to the excitation spectrum of $Gd_2O_3:Eu^{3+}$ obtained by using aqueous ammonia as the precipitant, that of sample using ammonium bicarbonate as the precipitant slightly shifts to left, which may be caused by

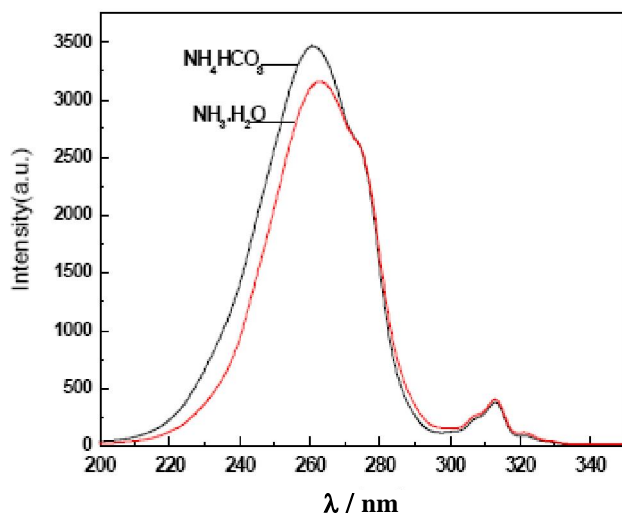


Figure 6 : Excitation spectra of samples obtained by using different precipitant

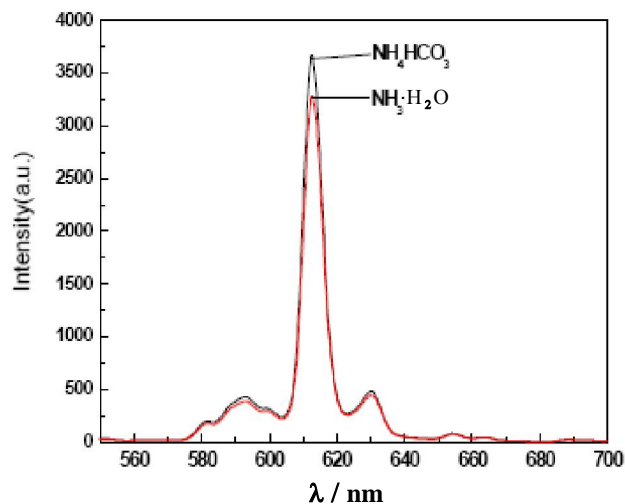


Figure 7 : Emission spectra of samples obtained by using different precipitant

the different size and morphology of particles.

The emission spectra of samples $Gd_2O_3:Eu^{3+}$ excited by 261 nm UV light are shown in Figure 7. It can be seen that the kind of precipitants has little effect on the shape and position of emission peaks, the main emission peak is all at 613 nm, which is ascribed to the ${}^5D_0 \rightarrow {}^7F_2$ hypersensitive transition of Eu^{3+} , resulting in a red emission^[9]. Moreover, some weak emission peaks can be observed, 582 nm (${}^5D_0 \rightarrow {}^7F_0$), 588 nm, 593 nm, 600 nm (${}^5D_0 \rightarrow {}^7F_1$) and 631 nm (${}^5D_0 \rightarrow {}^7F_3$), which are ascribed to the characteristic transitions of Eu^{3+} ^[10]. The kind of precipitants has some effect on the intensity of emission peaks (as shown in Figure 9). The peak intensity of the sample using ammonium bicarbonate as the precipitant is relatively strong. This is may be due to the fact that $Gd_2O_3:Eu^{3+}$ obtained using ammonium bicarbonate as the precipitant has more perfect crystallization (as shown in Figure 4(b)) and bigger length-diameter ratio, which reduce the chance of non-radiation transition.

CONCLUSION

Using aqueous ammonia as the precipitation agent, red-emitting phosphors $Gd_2O_3:Eu^{3+}$ was synthesized by hydrothermal method. The hydrothermal precursor is hexagonal $Gd(OH)_3$, pure cubic phase $Gd_2O_3:Dy^{3+}$ can be obtained after the precursor was calcined at 800 °C for 2h. $Gd_2O_3:Eu^{3+}$ particles are basically short bar in shape with small slenderness ratio, the diameter is about 100 nm~500 nm and the length is about 300 nm~1 μm. The main emission peak of $Gd_2O_3:Eu^{3+}$ is at about 613 nm, resulting in a red emission. When ammonium bicarbonate was used as the precipitation agent, the hydrothermal precursor is orthorhombic $Gd_2(CO_3)_3 \cdot xH_2O$, pure cubic phase $Gd_2O_3:Dy^{3+}$ can be obtained after the precursor was calcined at 800° for 2h. $Gd_2O_3:Eu^{3+}$ particles are basically long strips in shape with big slenderness ratio, the diameter is about 100 nm~1 μm and the length is about 1~9 μm. The main emission peak of $Gd_2O_3:Eu^{3+}$ is also at about 613 nm, but the intensity is higher than that of $Gd_2O_3:Eu^{3+}$ obtained using aqueous ammonia as the precipitant.

REFERENCES

- [1] C.C.Lin, K.M.Lin, Y.Y.Li, et al; J.Lumin., **126(2)**, 795-799 (2007).
- [2] Y.C.Kang, H.S.Roh, S.B.Park; J.Electrochem.Soc., **147(4)**, 1601-1603 (2000).
- [3] T.L.Phan, M.H.Phan, N.Vu, et al; Phys.Status Solidi A, **201(9)**, 2170-2174 (2004).
- [4] G.Jia, K.Liu, Y.Zheng, et al; J.Phys.Chem.C, **113(25)**, 6050-6055 (2009).
- [5] G.X.Liu, G.Y.Hong, J.X.Wang, et al; J.Alloys Compd., **432(1-2)**, 200-204 (2007).
- [6] S.W.Li, H.W.Song, H.Q.Yu, et al; J.Lumin., **122**, 876-878 (2007).
- [7] S.Zhang, G.X.Liu, X.T.Dong, et al; Chem.J.Chin. Univ., **30(1)**, 7-10 (2009).
- [8] Q.H.Yu, X.B.Li; J.Chin.Soc.Rare Earths, **11(2)**, 171-173 (1993).
- [9] Y.Q.Zhai, Z.H.Yao, M.D.Qiu, et al; Indian J.Chem., **43(A)**, 71-75 (2007).
- [10] L.D.Sun, C.Qian, C.S.Liao, et al; Solid State Commun., **119(6)**, 393 (2001).